Taylor & Francis
Taylor & Francis Group

Quantum control and quantum control landscapes using intense shaped femtosecond pulses

M. WOLLENHAUPT*, A. PRÄKELT, C. SARPE-TUDORAN,
D. LIESE and T. BAUMERT

University of Kassel, Institute of Physics,
Center for Interdisciplinary Nanostructure Science and Technology (CINSaT),
Heinrich-Plett-Str. 40, D-34132 Kassel, Germany

A hitherto not considered physical mechanism of quantum control with intense shaped femtosecond laser pulses is investigated. Phase modulated pulses are used to exert control on the strong-field ionization of potassium atoms. We use a sinusoidal phase modulation function to manipulate the intensity of the Autler–Townes (AT) components in the photoelectron spectrum. The effect of all sine parameters is studied systematically. In addition, controllability is investigated using parameterized pulse shapes to generate a two-dimensional quantum control landscape. Our results show that the selective population of dressed states is the underlying strong-field physical mechanism. Due to its robustness with respect to the laser parameters, the selective dressed state population is an important general control mechanism.

1. Introduction

Quantum control opens new perspectives in many fields of physics with applications ranging from laser science, quantum optics, atomic and molecular physics, solid state physics, photochemistry to biophysics or quantum computing due to the ability to manipulate quantum systems in a predefined way using shaped laser pulses. Various quantum control schemes have been proposed and experimentally demonstrated, which are reviewed in [1–5], examples of which are the Brumer–Shapiro scheme [6] and the Tannor–Kosloff–Rice scheme [7]. Despite their generality, most of these schemes are operative in the weak-field regime. An alternative approach based on adaptive pulse manipulation was suggested by Judson and Rabitz [8]. The use of pulse-shaping techniques [9] together with closed loop adaptive feedback learning algorithms enabled laboratory implementations of this idea to optimize a huge variety of physical observables [10–15]. However, in many cases it was found intricate to deduce the underlying physical mechanism from the

---

*Corresponding author. Email: wollenha@physik.uni-kassel.de

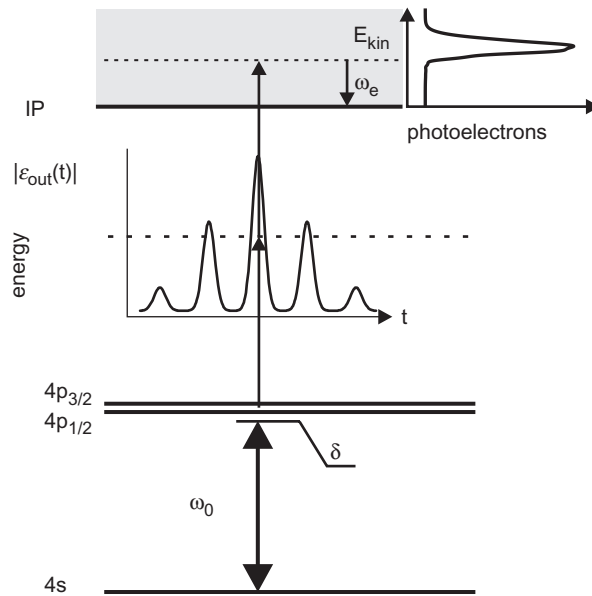Figure 1. Energy level diagram for excitation of K atoms. Shaped laser pulses with the envelope $|\mathcal{E}_{out}(t)|$ and a carrier frequency ω_0, slightly detuned from the resonance frequency, create a coherent superposition of the $4s$ and the upper $4p$ states. Photoelectrons with a kinetic energy $E_{kin} = \hbar\omega_e$ from simultaneous two-photon ionization are measured.

electrical fields obtained by this procedure. Therefore, the emphasis of this contribution is on the analysis of the underlying physical mechanisms in particular when intense laser fields are employed. Here, we investigate quantum control on potassium atoms, excited by intense phase modulated laser pulses. Atoms serve as a model system and can be viewed as an approximation to more complex situations. In our experiments, the K $4p \leftarrow 4s$ transition is coherently excited with phase modulated femtosecond laser pulses and subsequently ionized with the same pulse in a two-photon process (cf. figure 1). The resulting photoelectrons are detected with energy resolution to probe the dressed state population via the intensity of the Autler–Townes components. We use sinusoidal phase modulation functions in frequency domain since the corresponding pulses in time domain provide pulse sequences with well defined relative phases. The importance of the relative phase in experiments using optical pulse sequences was demonstrated in the mid-1980s using cw radiation [16–18]. Nowadays, sinusoidal phase modulation is a standard tool in quantum control experiments [19–21] and serves as a prototype for more complex phase functions.

2. Excitation and ionization scheme

In this section we present the excitation/ionization scheme of potassium atoms used in our experiment. Figure 1 shows the excitation scheme of our experiment.

The same shaped pulse is used to drive the neutral dynamics and also ionize the excited state potassium atoms. Our experiments are modelled theoretically by solving the time dependent Schrödinger equation for the light induced neutral atomic dynamics in order to consider strong-field effects using the short time propagator method as also applied in [21]. Photoionization is treated using perturbation theory since the neutral-to-ionic transitions are usually much weaker than resonant atomic transitions. The amplitudes $c(\omega_e)$ for photoelectrons with a kinetic energy of $\hbar\omega_e$ from the ionization of the 4p excited state read [22, 23]

$$c(\omega_e) = \int_{-\infty}^{\infty} c_b(t) E^2(t) e^{i(\omega_e + \omega_{IP} - \omega_{4p})t} \, dt, \tag{1}$$

where $c_b(t)$ describes the time dependent excited state amplitude. From equation (1) it is seen that the amplitudes $c(\omega_e)$ are the Fourier transform of the excited state amplitude $c_b(t)$ windowed by the square of the electrical field $E^2(t)$. In that sense $c_b(t)$ maps the transient population of the 4p state and the quantum mechanical phase information of the excited state amplitudes leaves a fingerprint in the photoelectron spectrum. In order to model the experimental results (section 4) we consider both the $s_{1/2} \rightarrow p_{1/2}$ and $s_{1/2} \rightarrow p_{3/2}$ transitions for linear polarized laser light. The unmodulated field $\mathcal{E}_{in}(t)$ envelope is obtained from the measured spectrum allowing for a residual, uncompensated linear chirp. The field $\mathcal{E}_{in}(t)$ is phase modulated in frequency domain to calculate $\mathcal{E}_{out}(t)$.

2.1 *Sinusoidal phase modulation*

In order to discuss the physical mechanism of quantum control using sinusoidal spectral phase modulation, some time domain properties of the modulated pulses are briefly summarized. We start with the unmodulated electrical field $\mathcal{E}_{in}(t)$ envelope. The phase modulation function in frequency domain reads

$$\varphi(\omega) = e^{i A \sin[(\omega - \omega_{ref}) \cdot T + \phi]}, \tag{2}$$

where A describes the amplitude of the phase modulation function, T the frequency of the sinusoidal oscillation, ω_{ref} the origin of the sine function on the phase mask and ϕ an absolute phase offset. The modulated electrical field envelope $\mathcal{E}_{out}(t)$ in time domain reads [21]

$$\mathcal{E}_{out}(t) = \sum_{n=-\infty}^{\infty} J_n(A) \, \mathcal{E}_{in}(t + nT) \, e^{in(\Delta\omega T + \phi)}, \tag{3}$$

where J_n describes the Bessel function of the first kind and order n, and $\Delta\omega = \omega_0 - \omega_{ref}$ describes the difference between the laser carrier frequency ω_0 and the reference frequency of the phase modulation function ω_{ref}. Thus, sinusoidal phase modulation in frequency domain creates a pulse sequence in time domain (cf. figure 1) with well defined relative phases.
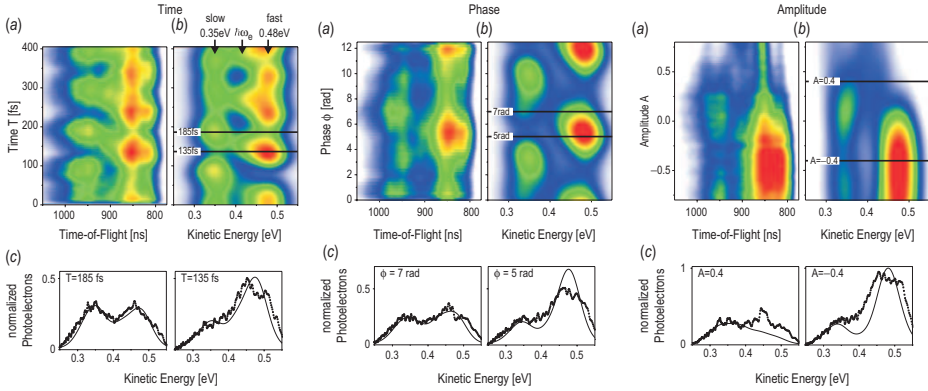
Figure 2. Photoelectron spectra for the variation of the time separation of the subpulses T (time), the absolute phase of the sine function ϕ (phase) and the modulation amplitude A (amplitude). In each panel (*a*) shows the measured photoelectron spectra and (*b*) the simulations. The lower panels (*c*) and (*d*) show sections through the measured (dotted lines) and calculated (bold lines) photoelectron distributions.

3. Experimental

The experiments were carried out in a high-vacuum chamber where a beam of atomic potassium K (4*s*) intersects perpendicularly with the femtosecond laser pulses leading to photoionization. The released photoelectrons are detected employing a kinetic energy time-of-flight electron spectrometer with an energy resolution of 25 meV at a kinetic energy of 1 eV. The 785 nm, 30 fs FWHM laser pulses are provided by an amplified 1 kHz Ti:sapphire laser system and phase modulated using a home-built liquid crystal pulse shaper [24]. The sinusoidally modulated pulses with a typical energy of 0.25 μJ are focused with a 30 cm lens into the interaction region.

4. Results

In this section we present the photoelectron spectra obtained by variation of the time separation of the subpulses T, the absolute phase of the sine function ϕ and the modulation amplitude A (cf. figure 2). The reference frequency ω_{ref} corresponds to a wavelength of 785 nm.

4.1 *Variation of the time T*

Figure 2 (Time) shows a false colour representation of the measured (*a*) and simulated (*b*) photoelectron spectra where the parameter T is varied from 0 to 405 fs in steps of $\Delta T = 5$ fs. For each value of T a time-of-flight spectrum was measured. The splitting of the two peaks in the photoelectron spectrum at around 0.35 eV (slow photoelectrons) and 0.48 eV (fast photoelectrons) of about 130 meV

is due to the AT effect [25] that maps the corresponding dressed state population. The intensities of both the slow and fast photoelectrons oscillate with variation of T with a period of about 100 fs. The oscillation of the slow photoelectrons is shifted by 50 fs with respect to the oscillation of the fast photoelectrons. It is seen from the photoelectron distribution that by variation of T either dressed state can be selectively populated. Sections through the photoelectron distribution along the energy axis for T = 135 fs and T = 185 fs yield the photoelectron spectra shown in figure 2(*c*). The comparison with the calculated photoelectron spectra shows good agreement. The spectrum at T = 135 fs demonstrates the selective population of the upper dressed state.

4.2 *Variation of the phase ϕ*

Figure 2 (Phase) shows the measured (*a*) and simulated (*b*) photoelectron spectra upon variation of the absolute phase ϕ of the sinusoidal modulation in the range 0–12.25 rad for fixed values of $A = 0.17$ and T = 55 fs. With variation of ϕ, the intensity distribution periodically changes the intensity of the slow and the fast photoelectrons. Figure 2(*c*) shows sections along the kinetic energy axis at $\phi = 7$ rad and $\phi = 5$ rad. At $\phi = 5$ rad, fast photoelectrons are produced with more efficiency which corresponds to the selective population of the upper dressed state during the laser pulse. The period of the oscillatory dressed state population upon variation of ϕ is 2π. This property is not related to the atomic system but is a consequence of the 2π periodicity of the phase mask.

4.3 *Variation of the amplitude A*

Figure 2 (Amplitude) shows the measured (*a*) and simulated (*b*) photoelectron spectra upon variation of the parameter A within the range -0.8 to 0.8 for fixed values of $\phi = 1.7$ rad and T = 55 fs. Sections through the photoelectron distributions shown in figure 2(*c*) at $A = 0.4$ (left) and $A = -0.4$ (right) are plotted to demonstrate the agreement between the experimental results and the simulated photoelectron spectra. For negative modulation amplitudes the upper dressed state is selectively populated with high efficiency showing little modulation upon changes of the amplitude. For positive values of A both dressed states are populated approximately equally.

4.4 *Quantum control landscape*

So far, the photoelectron spectra were investigated as a function of a single parameter. The full picture of attainable control is obtained when all relevant control parameters are varied and a quantitative fitness parameter for optimal control is defined. In this spirit, Rabitz recently suggested [26] obtaining a deeper insight into optimal control by exploring so-called quantum control landscapes, i.e. by the analysis of the topology of the search space for the optimal pulse shape. Generally, the high dimensionality of this space precludes its characterization in realistic experiments. However, we reduce the parameter space by utilizing para-meterized pulse shapes, e.g. the sine function, to approach such a quantum control
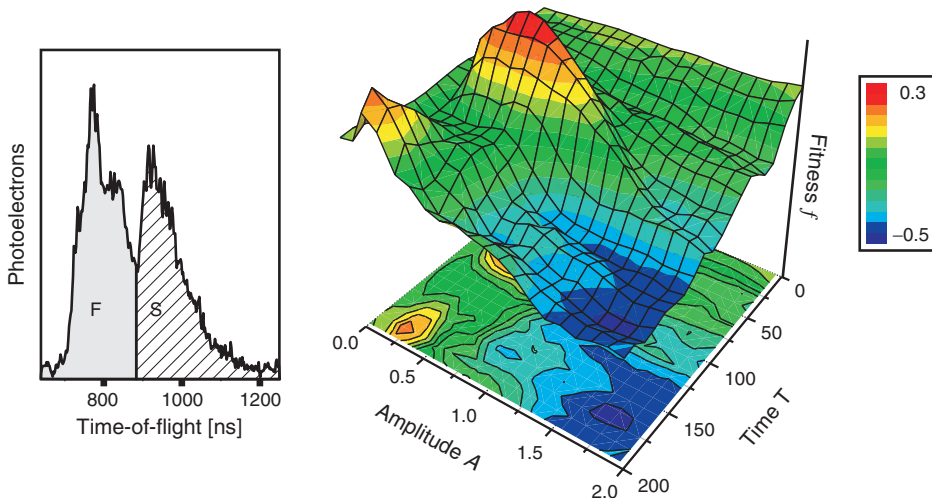
Figure 3. Left: the AT-photoelectron spectrum is divided into the slow (S) and fast (F) photoelectrons to map the topology of the parameterized control space spanned by the amplitude A and the delay time T for a fixed absolute phase of $\phi = 1.6$. Right: three-dimensional representation of the measured fitness function $f = (F - S)/(F + S)$.

landscape experimentally. Here we use the contrast of the integrated signal of the slow photoelectrons (S) versus the respective signal of the fast photoelectrons (F) as shown in figure 3 (left) as a fitness quantity. The parameters A and T of the sine function are varied in the measurement. A three-dimensional representation of the measured fitness function $f = (F - S)/(F + S)$ is shown in figure 3 (right). Even for the two-dimensional parameter space, the control landscape displays a complicated structure. However, areas of selective population of dressed states – showing up as the maxima ($f = 0.3$) and minima ($f = -0.5$) in figure 3 (right) – can be identified. In particular, at $A = 1.5$ and $T = 175\,\text{fs}$ a broad area of lower dressed state population is found whereas two localized areas of upper dressed state populations are observed (maxima in figure 3).

5. Discussion

In this section the atomic dynamics induced by sinusoidally phase modulated 30 fs (FWHM) laser pulses using the modulation parameters T = 100 fs, $\phi = \pi/2$, $A = 0.3$ and $\Delta\omega = \pi/50$ fs^{-1} is investigated. In order to depict the underlying physical mechanisms we consider the resonant excitation of a two-level atom. In figure 4(*a*) the time dependent Rabi frequency $\Omega(t)$ – which is proportional to the driving field envelope $\mathcal{E}(t)$ – and the temporal phase $\chi(t)$ are depicted. The envelope of the modulated electrical field $|E(t)|$ consists of a sequence of five subpulses separated by 100 fs. We first discuss the dynamics of the bare state population induced by each subpulse as shown in figure 4(*b*). The first subpulse ($n = 2$) leaves the ground state
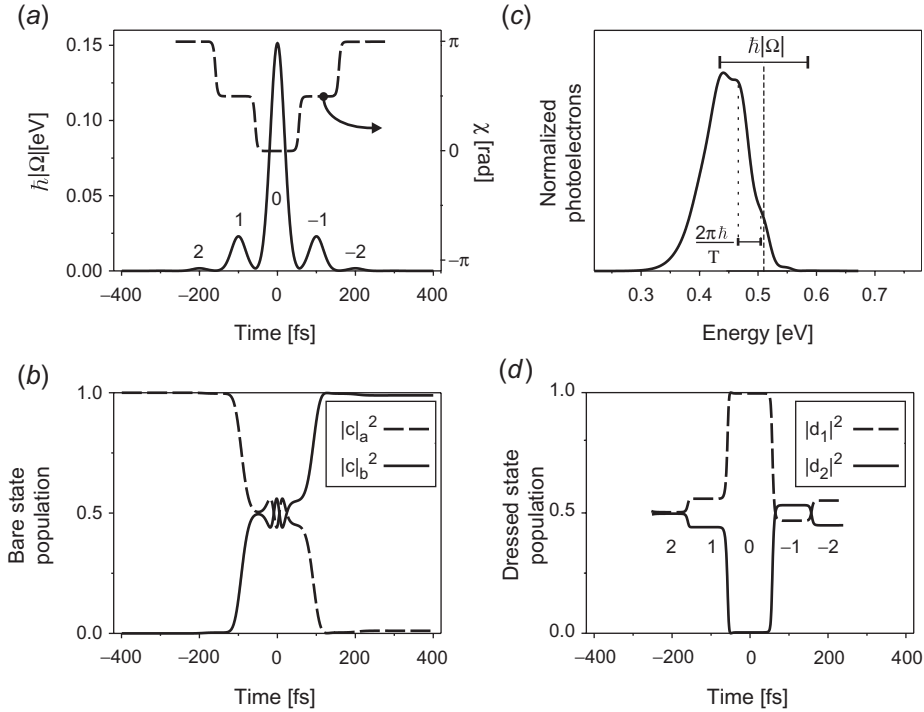
Figure 4. Simulation for resonant strong-field excitation using a sinusoidal phase modulated 30 fs FWHM Gaussian laser pulse. The modulation parameters are $A = 0.3$, $T = 100$ fs, $\phi = \pi/2$ rad and $\Delta\omega = \pi/50$ fs^{-1}. (*a*) Envelope of the electrical field $|\mathcal{E}(t)|$ in units of the AT splitting $\hbar|\Omega(t)| = |\mu\mathcal{E}(t)|$ (bold, left scale) and temporal phase $\chi(t)$ of the electric field (dashed, right scale). The subpulses are indicated with labels from $n = 2$ to -2. (*b*) Time evolution of the bare state population (ground state $|c_a|^2$ dashed, and excited state $|c_b|^2$ bold). (*c*) Simulated photoelectron spectrum: the dashed line indicates the kinetic energy of weak-field photoionization $\hbar\omega_e$ and the bar shows the AT splitting at the most intense subpulse ($n = 0$, compare value of $\hbar|\Omega(t)|$ in (a) at $t = 0$). (d) Population of the dressed states (lower state $|d_1|^2$ dashed, and upper state $|d_2|^2$ bold).

population unchanged. The second subpulse ($n = 1$) has a pulse area of $\pi/2$, leaving the system in a coherent superposition of both states with a population of $|c_a|^2 = |c_b|^2 = 0.5$. The third subpulse ($n = 0$) has the highest intensity but leaves the population unchanged (cf. figure 4*b* at $t \approx 0$). It was demonstrated in [27] that for certain relative phases of two pulses within a sequence, even resonant intense femtosecond pulses do not affect the population of an atom prepared in a superposition state, but rather control the quantum mechanical phase of both states. The fourth subpulse ($n = -1$) is in phase with the second subpulse ($n = 1$) and therefore continues the time evolution induced by the second subpulse. Next, we use the dressed state picture [17, 28, 29] to analyse the light induced dynamics (figure 4*d*) since the measured photoelectron spectra reveal the population of the dressed states. During the first subpulse, both dressed states are equally populated $|d_1|^2 = |d_2|^2 = 0.5$. Since the first subpulse creates a superposition state, the second

subpulse permits us to exert control on the population of the dressed states. This subpulse prepares the system in a state with $|c_a|^2 = |c_b|^2 = 0.5$. Due to the phase jump of $-\pi/2$ at -50 fs, selective population of the lower dressed state is achieved during the third subpulse. Because this subpulse has the highest intensity, two-photon ionization is most probable. As a consequence, the photoelectron spectrum maps the lower dressed state as seen in figure 4(*c*). By variation of the relative phases – for instance due to the choice of other parameters of the modulation function – the upper dressed state is selectively populated.

6. Conclusions

We investigated the physical mechanism of strong-field quantum control on an atomic model system for sinusoidal phase modulated femtosecond laser pulses. Sinusoidal phase modulation serves as a prototype for more complex pulse shapes. In order to study how quantum control is exerted with sinusoidal modulation, the sine parameters delay (T), phase (ϕ) and amplitude (*A*) were systematically varied. Efficient control of the AT components was achieved in each scan. Since the measured AT spectrum maps the dressed state population, the results show our ability to control the population of individual dressed states at will. The analysis of the measurements revealed that the precise control of the relative temporal phase of the pulses enabled the selectivity. For the first time the topology of a quantum control landscape was obtained by employing parameterized pulse shapes to reduce the dimensionality of the optimization problem. The observed control mechanism showed remarkable robustness with respect to the experimental implementation. Selective dressed state population is observed in the presence of serious deviations from the idealized physical picture such as off-resonant excitation, chirps or real (non-Gaussian) laser spectra (not discussed in this contribution). The robustness found experimentally is supported by simulations which indicate that the same mechanism is still operative when more than two atomic levels are considered. Therefore, we believe that the selective population of dressed states is a general principle in strong-field quantum control which is also applicable in larger systems.

References

[1] S.A. Rice, M. Zhao, *Optical Control of Molecular Dynamics* (Wiley-Interscience, New York, 2000).
[2] M. Shapiro, P. Brumer, *Principles of the Quantum Control of Molecular Processes* (Wiley-Interscience, Hoboken, 2003).

[3] M. Dantus, V. Lozovoy, Chem. Rev. **104** 1813 (2004).
[4] T. Brixner, T. Pfeifer, G. Gerber, et al., in *Femtosecond Laser Spectroscopy*, chapter 9: Optimal Control of Atomic and Molecular and Electron Dynamics with Tailored Femtosecond Pulses, edited by P. Hannaford (Kluwer, The Netherlands, 2004).
[5] M. Wollenhaupt, V. Engel, T. Baumert, Annu. Rev. Phys. Chem. **56** 25 (2005).
[6] P. Brumer, M. Shapiro, Chem. Phys. Lett. **126** 541 (1986).
[7] D.J. Tannor, R. Kosloff, S.A. Rice, J. Chem. Phys. **85** 5805 (1986).
[8] R.S. Judson, H. Rabitz, Phys. Rev. Lett. **68** 1500 (1992).
[9] A.M. Weiner, Rev. Sci. Instr. **71** 1929 (2000).
[10] T. Baumert, T. Brixner, V. Seyfried, *et al.*, Appl. Phys. B, **65** 779 (1997).
[11] D. Yelin, D. Meshulach, Y. Silberberg, Opt. Lett. **22** 1793 (1997).
[12] C.J. Bardeen, V.V. Yakolev, K.R. Wilson, *et al.*, Chem. Phys. Lett. **280** 151 (1997).
[13] A. Assion, T. Baumert, M. Bergt, *et al.*, Science **282** 919 (1998).
[14] R.J. Levis, G.M. Menkir, H. Rabitz, Science **292** 709 (2001).
[15] T. Brixner, G. Krampert, T. Pfeifer, *et al.*, Phys. Rev. Lett. **92** 208301 (2004).
[16] W.S. Warren, A.H. Zewail, J. Chem. Phys. **75** 5956 (1981).
[17] Y.S. Bai, A.G. Yodh, T.W. Mossberg, Phys. Rev. Lett. **55** 1277 (1985).
[18] E.T. Sleva, I.M. Xavier Jr., A.H. Zewail, J. Opt. Soc. Am. B **3** 483 (1986).
[19] N. Dudovich, B. Dayan, S.M. Gallagher Faeder, *et al.*, Phys. Rev. Lett. **86** 47 (2001).
[20] J.L. Herek, W. Wohlleben, R. Cogdell, *et al.*, Nature **417** 533 (2002).
[21] A. Präkelt, M. Wollenhaupt, C. Sarpe-Tudoran, *et al.*, Phys. Rev A **70** 063407-1 (2004).
[22] Ch. Meier, V. Engel, Phys. Rev. Lett. **73** 3207 (1994).
[23] D. Meshulach, Y. Silberberg, Phys. Rev. A **60** 1287 (1999).
[24] A. Präkelt, M. Wollenhaupt, A. Assion, *et al.*, Rev. Sci. Instr. **74** 4950 (2003).
[25] S.H. Autler, C.H. Townes, Phys. Rev. **100** 703 (1955).
[26] H.A. Rabitz, M.M. Hsieh, C.M. Rosenthal, Science **303** 1998 (2004).
[27] M. Wollenhaupt, A. Assion, O. Bazhan, *et al.*, Phys. Rev. A **68** 015401 (2003).
[28] B.W. Shore, *The Theory of Coherent Atomic Excitation*, Volume **1**: Simple Atoms and Fields (John Wiley, New York, 1990).
[29] M.O. Scully, M. Suhail Zubairy, *Quantum Optics* (University Press, Cambridge, 1997).